Journal of Medicinal Chemistry

ARTICLE

pubs.acs.org/jmc

Synthesis of a New [6]-Gingerol Analogue and Its Protective Effect with Respect to the Development of Metabolic Syndrome in Mice Fed a High-Fat Diet

Mayumi Okamoto,[*,†,∥] Hiroyuki Irii,[†] Yu Tahara,[‡] Hiroyuki Ishii,[§] Akiko Hirao,[‡] Haruhide Udagawa,[∥] Masaki Hiramoto,[∥] Kazuki Yasuda,[∥] Atsuo Takanishi,[§] Shigenobu Shibata,[‡] and Isao Shimizu[†]

[†]Department of Applied Chemistry, School of Advanced Science and Engineering, Waseda University, Shinjuku-ku, Tokyo, Japan

[‡]Department of Physiology and Pharmacology, School of Advanced Science and Engineering, Waseda University, Shinjuku-ku, Tokyo, Japan

[§]Faculty of Science and Engineering, Waseda University, Shinjuku-ku, Tokyo, Japan

[∥]Department of Metabolic Disorder, Diabetes Research Center, Research Institute, National Center for Global Health and Medicine, Shinjuku-ku, Tokyo, Japan

ABSTRACT:

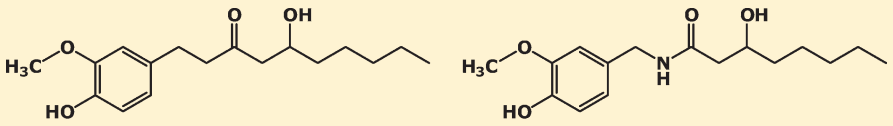

[6]-Gingerol (1) Aza-[6]-gingerol (2)

To determine the effects of a [6]-gingerol analogue (6G), a major chemical component of the ginger rhizome, and its stable analogue after digestion in simulated gastric fluid, aza-[6]-gingerol (A6G), on diet-induced body fat accumulation, we synthesized 6G and A6G. Mice were fed either a control regular rodent chow, a high-fat diet (HFD), or a HFD supplemented with 6G and A6G. Magnetic resonance imaging adiposity parameters of the 6G- and A6G-treated mice were compared with those of control mice. Supplementation with 6G and A6G significantly reduced body weight gain, fat accumulation, and circulating levels of insulin and leptin. The mRNA levels of sterol regulatory element-binding protein 1c (SREBP-1c) and acetyl-CoA carboxylase 1 in the liver were significantly lower in mice fed A6G than in HFD control mice. Our findings indicate that A6G, rather than 6G, enhances energy metabolism and reduces the extent of lipogenesis by downregulating SREBP-1c and its related molecules, which leads to the suppression of body fat accumulation.

INTRODUCTION

Metabolic syndrome comprises a constellation of metabolic abnormalities, including dyslipidemia (low HDL cholesterol, high LDL cholesterol, and high triglycerides), hyperglycemia, and elevated blood pressure, that increase the risk of developing cardiovascular disease. Two major underlying risk factors for metabolic syndrome are obesity and insulin resistance. Obesity results from an imbalance between fat synthesis (lipogenesis) and fat breakdown (lipolysis), both of which are regulated by the level and activity of molecules involved in carbohydrate and lipid metabolism. Thus, the molecules involved in these pathways are considered potential targets for the treatment of obesity and metabolic syndrome.[1,2] The expression of many lipogenic genes, such as acetyl-CoA carboxylase (ACC) and fatty acid synthase (FAS), is transcriptionally regulated by sterol regulatory element-binding protein 1 (SREBP-1). Suppression of lipogenic enzymes, including ACC and FAS, attenuates body fat accumulation.[1−4]

The prevalence of obesity is increasing globally; therefore, studies[1,2,5,6] of drugs and functional foods that regulate energy metabolism have been vigorously conducted with the aim of managing obesity and related diseases. Ginger (*Zingiber officinale* Roscoe) is widely used around the world in food as a spice. In addition, it has been an important ingredient in Chinese, Ayurvedic, and Tibb-Unani herbal medicines for the treatment of catarrh, rheumatism, nervous diseases, gingivitis, toothache, asthma, stroke, constipation, and diabetes.[7−9] The major chemical constituents of ginger rhizome are essential volatile oils and nonvolatile pungent compounds.[10,11] The volatile oil components are mainly various terpenoids. The nonvolatile compounds include gingerol [5-hydroxy-1-(4-hydroxy-3-methoxyphenyl)-3-decanone], shogaol [1-(4-hydroxy-3-methoxyphenyl)dec-4-en-3-one], paradol, and zingerone. Among them, gingerol and shogaol have been identified as the primary ginger-derived bioactive constituents.[12−14] Recently, a report demonstrated the hypoglycemic potential of ginger in streptozotocin (STZ)-induced diabetic rats treated with an aqueous extract of raw ginger daily for a period of 7 weeks; additionally, it showed that raw ginger was effective in reversing diabetic protein urination and loss of body weight observed in the diabetic rats.[15]

Received: May 25, 2011
Published: August 18, 2011

Scheme 1. Synthesis of 6G (1) (a) and A6G (2) (b)

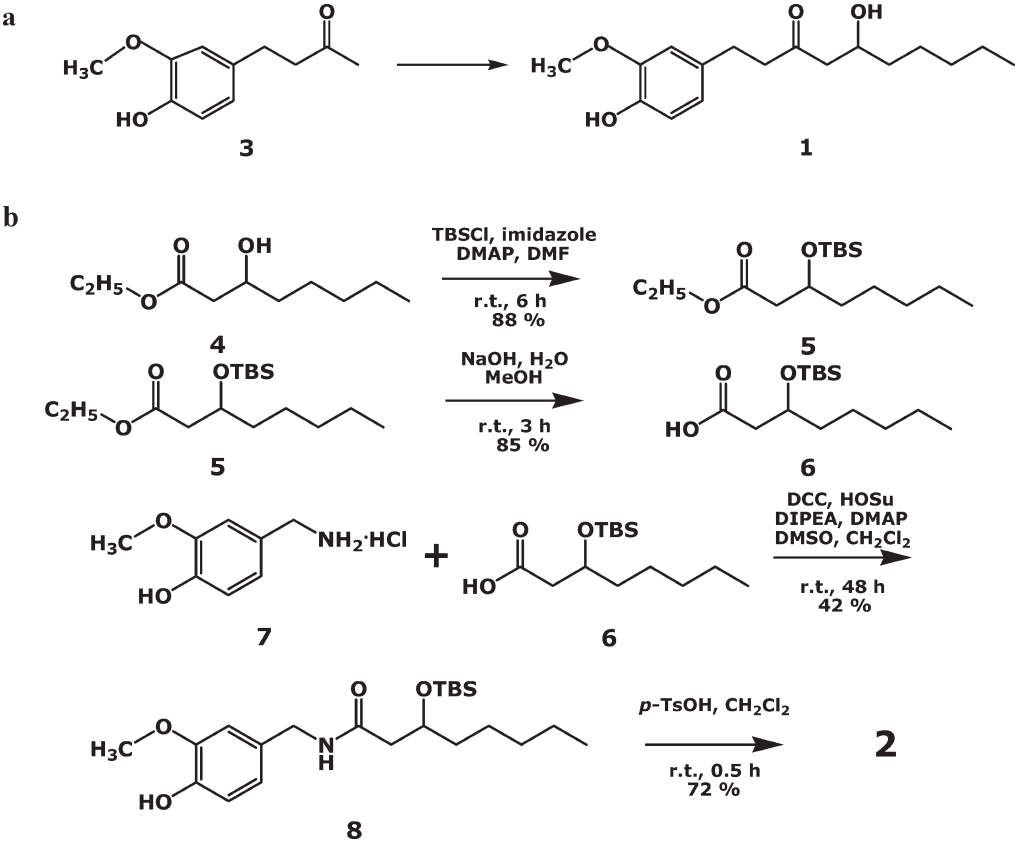

Gingerol and shogaol are known to activate transient receptor potential vanilloid-1 (TRPV1).[16] Therefore, gingerol and shogaol may be potentially valuable in inducing weight loss. The prototypical agonist of TRPV1 is capsaicin (8-methyl-*N*-vanillyl-*trans*-6-nonenamide), the pungent compound found in chili peppers. In fact, capsaicin is found to exert multiple pharmacological and physiological effects, including analgesic, anticancer, anti-inflammatory, antioxidant, and anti-obesity effects.[17] The important structural difference between capsaicin and gingerol or shogaol is the presence of an amide group in the former. It has been suggested that the amide group is responsible for the anti-obesity effects of capsaicin. Therefore, we synthesized A6G as a representative compound of gingerol containing an amide group.

^{1}H magnetic resonance imaging (MRI) offers several methods for obtaining separate fat and water images and allows quantification of fat volumes in anatomically distinct fat deposits noninvasively and simultaneously.[18−22] The MRI system is not invasive in itself, and this is an advantage over computed tomography (CT) where the experimental animal must be exposed to radiation.

In this study, we synthesized a chemical analogue of the gingerol (A6G) and examined it by comparing it with gingerol as a potential anti-obesity therapeutic agent. We also evaluated the effects of these compounds on energy metabolism-related molecules and found that A6G with an amide group suppressed body fat accumulation induced by a high-fat diet by down-regulating SREBP-1c and downstream molecules and stimulating the expenditure of energy in mice. Here, we have demonstrated that the daily intake of A6G rather than 6G could be a potentially effective and safe approach for preventing or attenuating obesity and metabolic syndrome.

RESULTS

Chemical Synthesis. Structural attributes of each analogue are presented in Scheme 1.

Effect of A6G on Fasting Blood Glucose. Blood glucose levels after mice had fasted for 12 h were measured 0, 9, 16, 23, 30, 44, 48, 57, 68, and 86 days after mice had been fed 6G or A6G. As shown in Figure 1a, the fasting blood glucose level prior to the treatments among the experimental groups varied within the normal physiological range, although the levels were significantly different among some of the groups. At the end of 86 days, mice fed HFD alone showed significant ($P < 0.001$) elevations in fasting blood glucose levels as compared with the pretreatment glucose levels or with those in the normal controls fed RC. Treatment of 6G or A6G with HFD produced a significant reduction ($P < 0.001$) in fasting blood glucose levels as compared with the controls fed a HFD. Moreover, at the end of the treatment, the serum glucose levels in the 6G- or A6G-treated groups were not significantly different from their pretreatment glucose levels or from those in the RC control group.

Effect of A6G on Body Weight. The changes in the mean body weight of the experimental groups of mice over the 12-week treatment period are shown in Figure 2b. There was no significant difference in the initial body weights and the body weights after 3 weeks [from 29.0 ± 0.5 to 30.3 ± 0.6 g ($n = 6$)] in the different groups. Animals treated with HFD alone exhibited significant increases in body weight (51.2 ± 2.7 g) as compared with their pretreatment values (29.8 ± 1.6 g) ($P < 0.001$) or with the control group receiving RC diet alone (45.0 ± 0.8 g) ($P < 0.001$). The HFD groups treated with 6G or

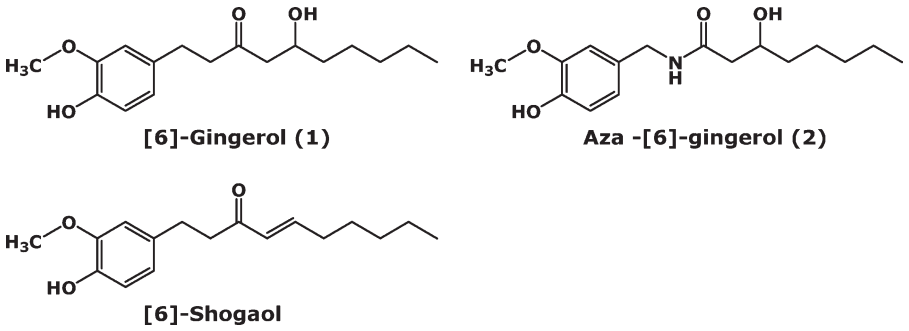

Figure 1. Structures of [6]-gingerol (6G) (**1**), aza-[6]-gingerol (A6G) (**2**), and [6]-shogaol (6S).

A6G showed significant reductions in body weight [from 51.2 ± 2.7 to 47.1 ± 1.1 g ($P < 0.001$) for 6G and from 51.2 ± 2.7 to 41.6 ± 0.2 g ($P < 0.001$) for A6G] compared with HFD-treated controls. Therefore, the body weights of the A6G-treated mice (41.6 ± 0.2 g) were not significantly different from those of the RC control mice after 86 days (45.0 ± 0.8 g) ($P = 0.07$).

Effect of A6G on VS and SC Fat Volumes. After treatment with each compound for 86 days, MRI was performed. Figure 3 shows a ^{1}H fat MRI image of representative different groups. Groups treated with HFD alone exhibited a significant increase (20.8 ± 1.7%) in percent body fat [visceral (VS) and subcutaneous (SC)] as compared with the RC control group (5.4 ± 1.7%) ($P < 0.001$). The HFD groups treated with 6G or A6G showed significant reductions in percent body fat [from 20.8 ± 1.7 to 10.9 ± 1.0% ($P < 0.001$) for A6G and from 20.8 ± 1.7 to 6.7 ± 0.8% ($P < 0.001$ for 6G] as compared with the HFD-treated controls, whereas the percent body fat of A6G-treated mice (6.7 ± 0.8%) was not significantly different from the RC control mice after 86 days (5.4 ± 1.7%) ($P = 0.41$).

Figure 4b shows the changes in the VS fat volumes of different groups under sacrificed conditions. The HFD animals treated with 6G or A6G showed a significant decrease [3.5 ± 0.2 g ($P < 0.01$) for 6G and 1.84 ± 0.2 g ($P < 0.001$) for A6G] in the VS fat volumes as compared with controls treated with HFD alone (5.03 ± 0.5 g). A significant difference was noted between the 6G group (3.5 ± 0.2 g) and the A6G group for VS fat weight (1.84 ± 0.2 g) ($P < 0.001$). No statistically significant difference was found between the adiposity volumes calculated via MRI and the adiposity volumes found at autopsy (for all, $P > 0.2$).

Effect of A6G on the Oral Glucose Tolerance Test. On days 92−94, OGTT was performed. Treatment with 6G or A6G significantly ($P < 0.001$) improved the glucose tolerance and inhibited the increase in postprandial glucose levels after glucose load intake in the groups fed HFD alone (Figure 4c).

Effect of A6G on Serum Hormones and Gene Expression in Adipose and Liver Tissue. Prior to the treatments with the compounds, the serum insulin concentration was not significantly different among the experimental groups. However, the groups treated with 6G or A6G showed a significant reduction in serum insulin levels ($P < 0.05$ for 6G; $P < 0.01$ for A6G) (Figure 5a) and serum leptin levels ($P < 0.01$) (Figure 5b) as compared with HFD-treated controls. Serum insulin and leptin concentrations were lower, but not significantly, in the A6G-treated groups than in the 6G-treated groups. Supplementation with 6G or A6G significantly reduced the level of mRNA expression of leptin (Figure 5c) and TNFα (Figure 5d) in

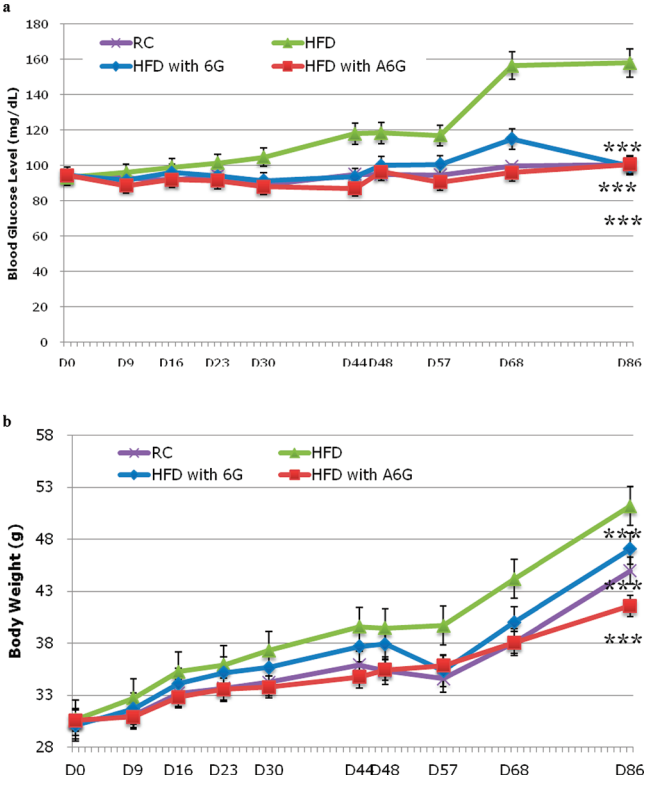

Figure 2. Effect of 6G or A6G treatment for 86 days on (a) fasting blood glucose level and (b) body weight in HFD-induced mice. Data are expressed as means ± standard error of the mean ($n = 5$ or 6; ***$P < 0.001$ vs HFD).

adipose tissue ($P < 0.01$). The level of mRNA expression of leptin was lower, but not significantly, in the A6G groups as compared to that in the 6G groups.

To elucidate the underlying mechanisms of the effects of A6G, we used real-time polymerase chain reaction (PCR) after mice had been fed for 86 days, during which time there were no significant differences in food intake among the HFD groups, to examine A6G-induced changes in gene expression in the liver. Supplementation with 6G or A6G caused insignificant decreases in the mRNA levels of ACC-1 and FAS, which are lipogenic enzymes in the liver, as compared with the respective levels in the HFD control group (Figure 6b,c). The mRNA levels of SREBP-1c, the master regulator of fatty acid synthesis,[23,24] were lower in the HFD group treated with A6G (Figure 6a).

A6G Attenuates TNFα-Mediated Downregulation of *adiponectin* Gene Expression. Marked reduction of the level of

dx.doi.org/10.1021/jm200662c |*J. Med. Chem.* 2011, 54, 6295–6304

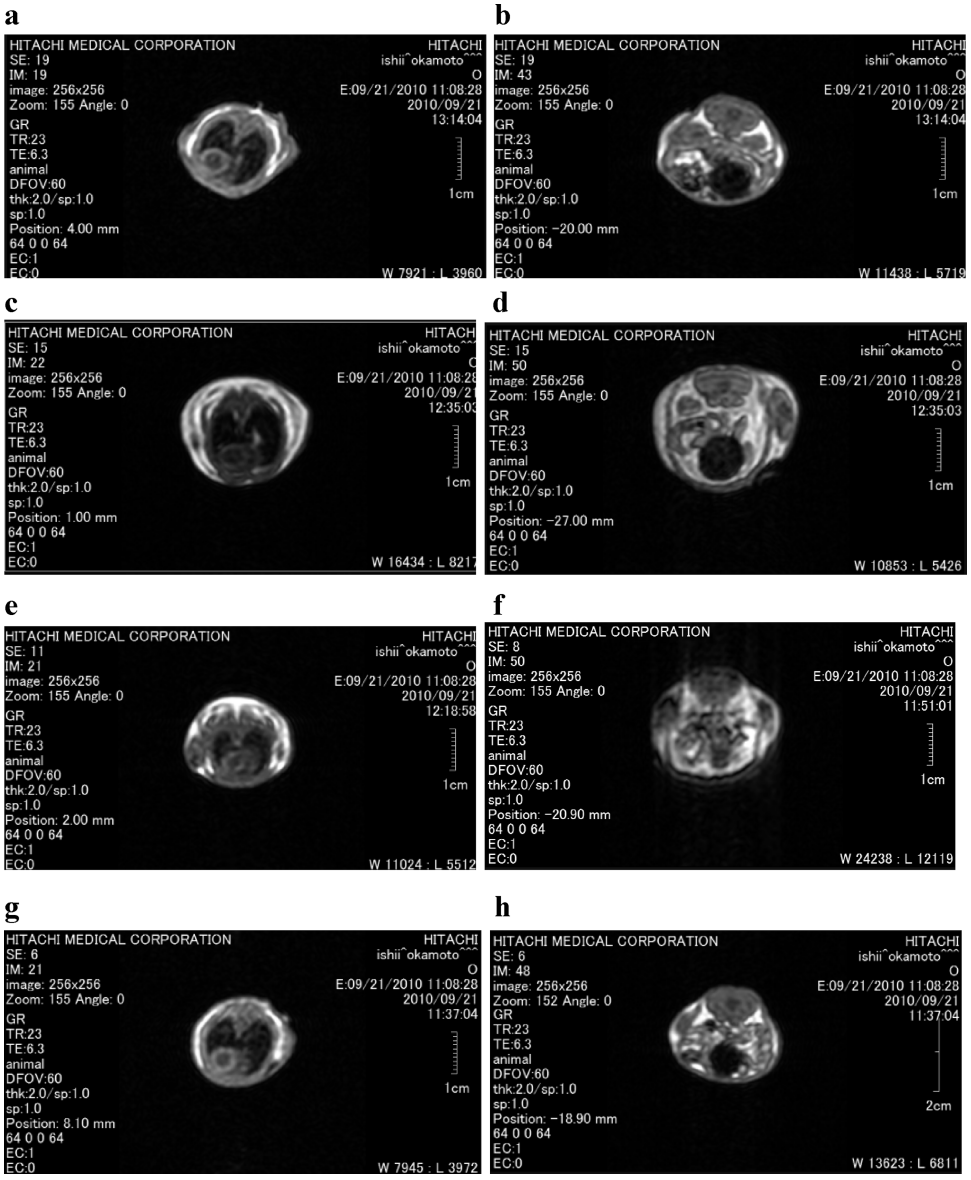

Figure 3. Axial images of mice fed RC (a and b), HFD (c and d), HFD with 6G (e and f), or HFD with A6G (g and h). Panels a, c, e, and g show subcutaneous fat (SC), and panels b, d, f, and h show visceral fat (VS).

adiponectin gene expression was observed after the administration of TNFα ($P < 0.0001$) (Figure 7) in adipocytes. In contrast, downregulation of *adiponectin* gene expression was significantly attenuated by pretreatment with 6G or A6G ($P < 0.01$ for 25 and 50 μM 6G, $P < 0.05$ for 25 μM A6G, and $P < 0.001$ for 50 μM A6G) (Figure 7) as well as with rosiglitazone ($P < 0.0001$). Furthermore, the *adiponectin* gene expression after pretreatment with 50 μM A6G (0.793 ± 0.14) was not significantly different from that after pretreatment with rosiglitazone (0.879 ± 0.21) ($P = 0.939$; Figure 7).

■ DISCUSSION

In this study, we examine the protective effects of 6G and A6G in mice fed a high-fat diet, a metabolic model of obesity and type 2 diabetes that is similar to human metabolic syndrome.[25] Because mice have metabolic patterns similar to those of humans, it is rational to use this disease model to examine the prophylactic effects of chronic treatment with 6G and/or A6G. To the best of our knowledge, this is the first study to use mice fed a high-fat diet to investigate the protective effects of gingerol derivatives in vivo.

Metabolic syndrome is a complex polygenic disorder resulting in part from the contribution of impaired insulin secretion and/or impaired insulin action on its receptors.[26] When carbohydrates are in short supply, or their breakdown is incomplete, fats become the preferred source of energy.[27] As a result, fatty acids are mobilized into the general circulation, leading to secondary triglyceridemia with increased levels of total serum lipids, including triglycerides, cholesterol, and phospholipids, leading to life-threatening lipid disorders.[28] The development of metabolic syndrome is influenced by a combination of genetic and environmental factors. Among the environmental factors, long-term high-fat intake has been most intensively studied because of its contribution to the development of metabolic syndrome in humans and rodents.[29] Apparently, a high proportion of daily energy

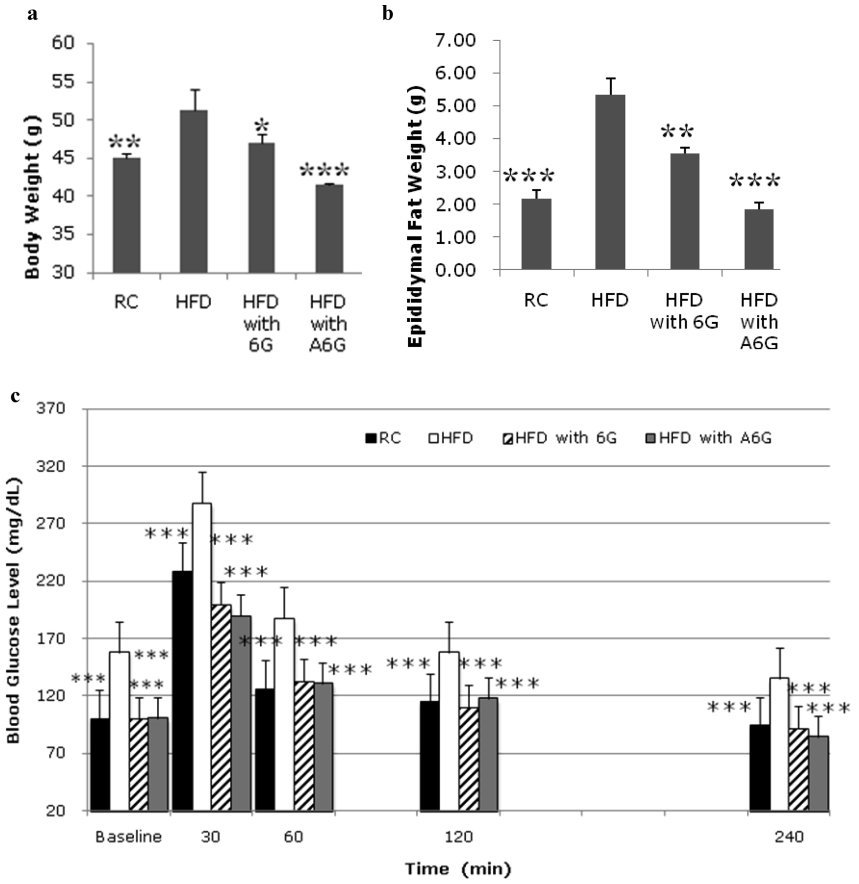

Figure 4. Effect of treatment with 6G or A6G for 86 days on (a) body weight, (b) epididymal fat weight, and (c) oral glucose tolerance. Data are expressed as means ± standard error of the mean (n = 5 or 6; $^{**}P < 0.01$ or $^{***}P < 0.001$ vs HFD).

derived from the fat component is a common situation in current lifestyles in most societies of the world. The high prevalence of metabolic disorders is probably related to abnormal blood profiles that may be due to the long-term effects of high-fat intake.[30]

Significant increases in body weight, serum glucose levels, and insulin levels along with reduced insulin sensitivity have been demonstrated in mice fed a high-fat diet.[14,31,32] This study reveals that 6G and A6G effectively suppressed body weight gain and body fat accumulation, lowered serum glucose and insulin levels, and increased insulin sensitivity upon concomitant administration along with high-fat diet.

The data obtained in this study are in agreement with a recent report that 6G significantly inhibited the TNFα-mediated downregulation of adiponectin gene expression in adipocytes.[13] In addition, we demonstrated that A6G significantly inhibited that process like 6G. Isa et al.[13] reported an upregulation of adiponectin by [6]-shogaol (6S) and 6G, the major components of *Z. officinale*. They also reported that 6S, but not 6G, possesses significant PPAR-γ agonistic activity. It is clear that the plasma adiponectin concentration and its mRNA expression level both undergo a reduction in obese and insulin-resistant states; it is therefore believed that the exogenous administration or upregulation of endogenous adiponectin by pharmacological intervention would improve insulin sensitivity, followed by an increase in the level of fatty acid oxidation and a decrease in serum triglyceride levels.[13] Thus, these latter findings strongly lend support to the results of our study involving mice treated with a high-fat diet, suggesting that the glucose-regulating and insulin-sensitizing effects of 6G and A6G can, at least in part, be attributed to PPAR-γ agonist activity and/or the upregulation of adiponectin.

We observed that 6G and A6G downregulated lipogenic enzymes, such as ACC-1 and FAS, in the liver. The expression of several lipogenic genes is regulated by SREBP-1c at the transcriptional level.[23,24] According to our findings, intake of A6G decreased SREBP-1c mRNA levels in the liver. Overall, our results suggest that A6G represses the lipogenic pathway by downregulating SREBP-1c, which leads to a reduction in the rate of accumulation of body fat.

Gingerols possess a labile hydroxyketo functional group, which renders them susceptible to transformation to less pungent compounds such as shogaols and zingerone at elevated temperatures.[12,33] The stability of 6G and 6S is significant and relevant as these substances are generally considered the main active constituents in ginger-based medicinal products. In the gastrointestinal tract, gingerols are exposed, in addition to acid, to digestive juices, containing pepsin in the stomach and pancreatin in the small intestine. Exposure of gingerols to these compounds could lead to considerable acid- and/or enzyme-catalyzed decomposition.[34] It is known that biotransformation of drugs in biological systems consists of reactions such as oxidation, reduction, hydrolysis, and conjugation of a drug or its metabolites, leading to activation or inactivation of the drug or formation of metabolites with pharmacological activities different from those of the parent drug. Isa et al.[13] reported that the two ginger-derived components have a potent and unique pharmacological function in 3T3-L1 adipocytes via different mechanisms. A recent study

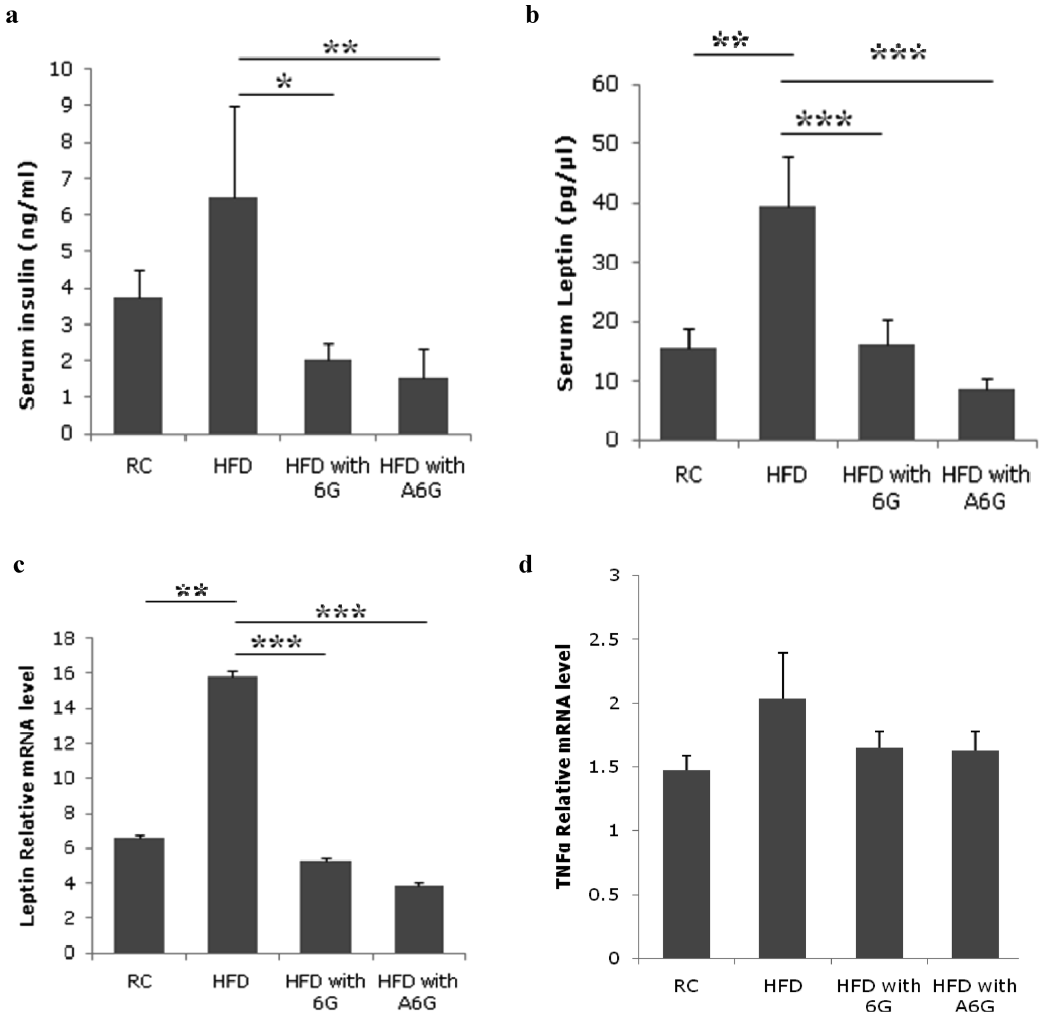

Figure 5. Effect of 6G or A6G on HFD-induced metabolic changes, (a) serum insulin and (b) leptin, and mRNA expression in adipose tissue of (c) leptin and (d) TNFα. Data are expressed as means ± standard error of the mean (n = 3−6; *P < 0.05, **P < 0.01, and ***P < 0.001 vs HFD).

demonstrated that ginger-derived components do have significant potency and act in a unique pharmacological manner that is responsible for the regulation of adipocyte function. Both 6S and 6G significantly inhibited TNFα-mediated downregulation of adiponectin expression in adipocytes. 6S, but not 6G, is a significant agonist for PPAR-γ. The significant upregulation of adiponectin observed after administration of 6S supports the finding that 6S inhibits TNFα-mediated downregulation of adiponectin expression by functioning as a PPAR-γ agonist. Ginger-derived components (6S and 6G) have a unique therapeutic potential that possibly may be used to regulate adipocyte function. These compounds can significantly inhibit TNFα-mediated downregulation of adiponectin in adipocytes, although they do so via different mechanisms.

We found that A6G was stable in simulated gastric fluid (pH 1) or 6 N HCl from 25 to 140 °C without degradation leading to the formation of shogaols. However, in simulated gastric fluid, 6G and 6S underwent first-order reversible dehydration and hydration reactions to form 6S and 6G, respectively. The presence of the hydroxyl moiety (6G) does not affect PPAR-γ activation, although it does contribute to the inhibition of TNFα-mediated JNK activation. In the absence of the hydroxyl moiety (6S), the compound is effective as a functional PPAR-γ agonist; however, there is diminished inhibitory activity of JNK activation.[13] In short, the structure, 6S or 6G, that possesses anti-obesity activity when administered orally remains unclear. Because A6G is a stable structure, we hope to elucidate the mechanisms of its anti-obesity effects in our future studies. In conclusion, the new [6]-gingerol analogue, A6G, which includes an amide group, revealed a remarkable protective effect against high-fat diet-induced metabolic disturbances by strongly suppressing body weight gain, hyperglycemia, and body fat accumulation by modulating fatty acid or glucose metabolism and insulin resistance conditions. Moreover, A6G remained stable in simulated gastric fluids (pH 1) at 37 °C. Thus, our findings suggest that A6G possesses potential therapeutic value and could potentially reduce the risk of obesity-associated disease, including type 2 diabetes. Further studies are being undertaken for achieving an in-depth understanding of the mechanism(s) underlying the glucose and lipid metabolism-regulating activities of A6G.

MATERIALS AND METHODS

All reagents and solvents were purchased commercially and used as received. ^{1}H NMR and ^{13}C NMR spectra were recorded with $CDCl_3$ as a solvent using tetramethylsilane as an internal standard on JEOL AL-400

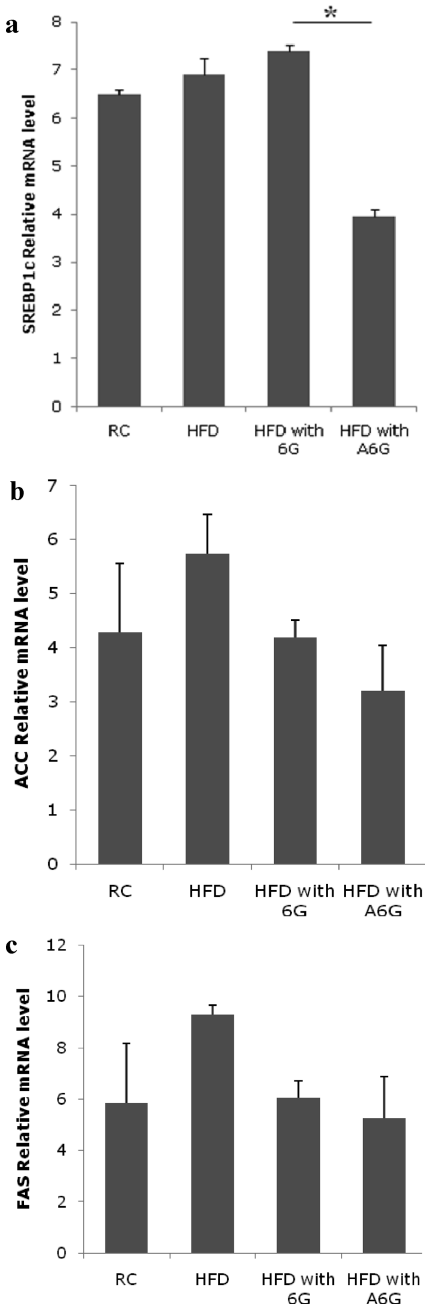

Figure 6. Effect of 6G or A6G on HFD-induced mRNA expression in liver of (a) SREBP-1c, (b) ACC, and (c) FAS. Data are expressed as means ± standard error of the mean (n = 3−6; *P < 0.05 vs HFD).

spectrometers. Multiplicities are indicated as br (broadened), s (singlet), d (doublet), t (triplet), q (quartet), or m (multiplet). Infared (IR) spectra were recorded on a JEOL JIR-WINSPECK 50 FT-IR spectrometer (ν_{max} in cm^{-1}). Bands are characterized as br (broad), s (strong), m (medium), or w (weak). High-resolution mass spectrometry (HRMS) spectra were recorded on a JMS-SX102A instrument (JEOL, Tokyo, Japan). Gas chromatographic analyses (GC) were conducted on a GC-4000 instrument (GL Sciences, Tokyo, Japan) equipped with an InsertCap 1 column [0.53 mm (inside diameter) × 30 m], using He as a carrier gas. Purity was determined by NMR and GC, and all compounds were confirmed to be >98% pure. [6]-Gingerol (6G) (**1**) was prepared as a racemic mixture according to a previously described method[35] (Scheme 1a). Synthesis of aza-[6]-gingerol (A6G) (**2**) was conducted by starting with ethyl 3-(*tert*-butyldimethylsilyloxy)octanoate **3**[36] as shown in Scheme 1b.

5-Hydroxy-1-(4-hydroxy-3-methoxyphenyl)-3-decanone (1). To a stirred solution of Zingerone (**3**, 1941 mg, 10 mmol) and *t*-BuOK (2805 mg, 25 mmol) in THF (100 mL) was added hexanal (1.48 mL, 12 mmol) at −78 °C. After 1.5 h, the reaction was quenched by the addition of saturated aqueous NH_4Cl. The mixture was extracted with ethyl acetate. The combined organic layer was washed with brine, dried over $MgSO_4$, filtered, and evaporated to dryness under reduced pressure. The crude product was purified by flash column chromatography (12.5% ethyl acetate/hexane) to provide **1** (2246 mg, 76%): ^{1}H NMR δ 0.88 (s, 3H), 1.21−1.53 (m, 8H), 2.48 (dd, 1H, J = 17.4 Hz, J = 8.9 Hz), 2.57 (dd, 1H, J = 17.4 Hz, J = 3.2 Hz), 2.77 (m, 4H), 2.93 (s, 1H), 3.88 (s, 3H), 4.02 (m, 1H), 5.56 (s, 1H), 6.67 (m, 2H), 6.83 (d, 1H, J = 8.0 Hz); ^{13}C NMR δ 14.0, 22.6, 25.1, 29.3, 31.7, 36.4, 45.4, 49.3, 55.9, 111.0, 114.3, 120.7, 132.0, 144.0, 146.4, 211.4; IR (neat) 3423.6 (br), 2931.7 (s), 2858.5 (m), 1704.6 (s), 1516.4 (s), 1272.1 (m), 1236.9 (m), 1154.1 (m), 1034.7 (m) cm^{-1}; HRMS (ESI) m/z calcd for $C_{16}H_{27}O_4$ (M) 294.1831, found 294.1825.

Ethyl 3-(*tert*-Butyldimethylsilyloxy)octanoate (5). To a stirred solution of dimethylaminopyridine (DMAP, 39.2 mg, 0.32 mmol), imidazole (0.871 g, 12.7 mmol), and *tert*-butyldimethylchlorosilane (1.45 g, 9.6 mmol) was added alcohol **4** (0.602 g, 3.2 mmol) in DMF (32 mL), and the mixture was stirred for 6 h. Saturated aqueous NH_4Cl was added to the reaction mixture, and the mixture was extracted with ether. The ethereal extract was washed with brine and a phosphate buffer solution, dried over anhydrous magnesium sulfate, filtered, and condensed in vacuo. The residue was chromatographed on silica gel with a 3% ethyl acetate/hexane solution as an eluent to provide silyl ether **5** (0.851 g, 88%): ^{1}H NMR δ 0.035 (s, 3H), 0.059 (s, 3H) 0.87 (s, 9H), 0.89 (t, 3H, J = 6.8 Hz), 1.27 (t, 3H, J = 7.1 Hz), 1.3−1.5 (m, 8H), 2.40 (dd, 1H, J = 14.6 Hz, J = 5.9 Hz), 2.42 (dd, 1H, J = 14.6 Hz, J = 7.1 Hz), 4.11 (m, 1H), 4.12 (q, 2H, J = 7.1 Hz); ^{13}C NMR δ −4.75, −4.47, 14.0, 14.2, 18.1, 22.7, 24.7, 25.9, 31.9, 37.6, 42.8, 60.3, 69.5, 172.0; IR (neat) 2956.8 (m), 2930.5 (s), 2857.9 (m), 1739.1 (s), 1255.4 (w), 1094.0 (w), 836.3 (m), 775.6 (w) cm^{-1}; HRMS (ESI) m/z calcd for $C_{16}H_{34}O_3SiNa$ $(M + Na)^+$ 325.2175, found 325.217.

3-(*tert*-Butyldimethylsilyloxy)octanoic Acid (6). To a solution of sodium hydroxide (0.5 g, 12.5 mmol) in water (8 mL) was added ester **5** (0.756 g, 2.5 mmol) in methanol (2 mL), and the mixture was stirred for 24 h at room temperature. Dilute hydrochloric acid (1 M) was added to the mixture, and the mixture was extracted with ether. The combined organic layer was dried over anhydrous magnesium sulfate, filtered, and condensed in vacuo. The residue was chromatographed on silica gel with a solution of 15% ethyl acetate in hexane as an eluent to provide **6** (0.584 g, 85%): ^{1}H NMR δ 0.104 (s, 3H), 0.113 (s, 3H), 0.89 (t, 3H, J = 5.8 Hz), 0.90 (s, 9H), 1.3−1.5 (m, 8H), 2.49 (dd, 1H, J = 15.1 Hz, J = 5.3 Hz), 2.57 (dd, 1H, J = 15.1 Hz, J = 5.1 Hz), 4.11 (quintet, 1H, J = 6.0 Hz); ^{13}C NMR δ −4.88, −4.56, 14.0, 18.0, 22.6, 24.7, 25.7, 31.8, 37.3, 42.2, 69.4, 177.5; IR (neat) 2956.9 (m), 2930.7 (m), 2858.7 (m), 1713.3 (s), 1255.4 (w), 1094.0 (w), 836.3 (m), 775.6 (w) cm^{-1}; HRMS (ESI) m/z calcd for $C_{14}H_{30}O_3SiNa$ $(M + Na)^+$ 297.1862, found 297.1869.

3-(*tert*-Butyldimethylsilyloxy)-*N*-(4-hydroxy-3-methoxybenzyl)octanamide (8). To a stirred solution of carboxylic acid **6** (0.150 g, 0.55 mmol) in dichloromethane (2.5 mL) were added *N*,*N*-dimethyl-4-aminopyridine (6.84 mg, 0.056 mmol), *N*,*N*-dicyclohexylcarbodiimide (0.227 g, 1.1 mmol), *N*-hydroxysuccinimide (0.127 g, 1.1 mmol), *N*,*N*-diisopropylethylamine (0.29 mL, 1.65 mmol), and ammonium chloride **7** (0.126 g, 0.67 mmol) in *N*,*N*-dimethyl sulfoxide (2.5 mL), and the mixture was stirred for 48 h. A saturated aqueous NH_4Cl solution was added to the mixture, and the mixture was extracted with ether. The ethereal extract was dried over anhydrous magnesium sulfate, filtered, and condensed in vacuo. The residue was chromatographed on silica gel with a solution of 15% ethyl acetate in

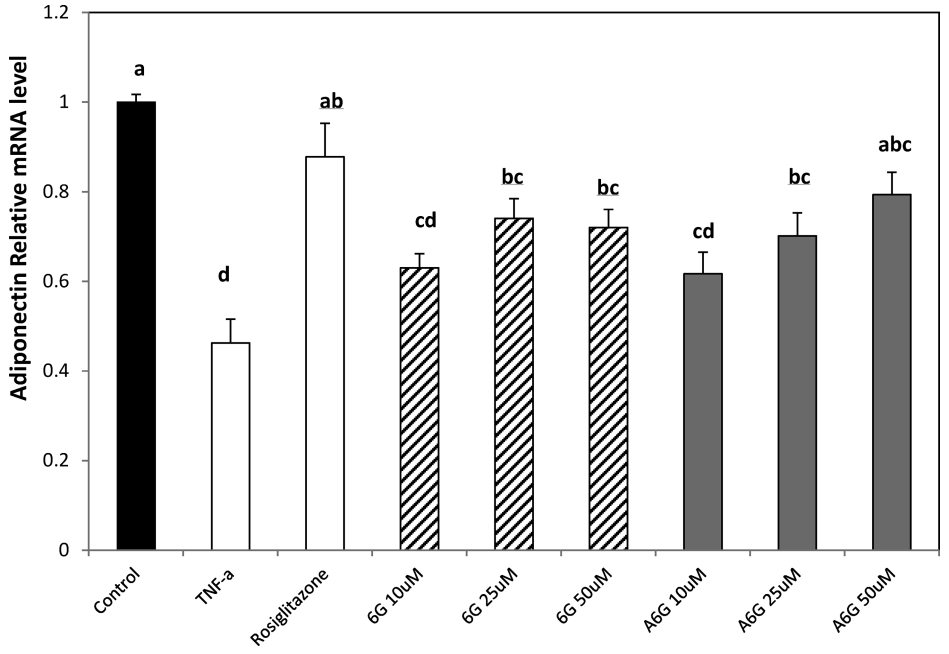

Figure 7. Inhibitory effect of 6G or A6G on the TNFα-mediated downregulation of *adiponectin* gene expression in 3T3-L1 adipocytes. Mice fed 6G (10, 25, and 50 μM), A6G (10, 25, and 50 μM), rosiglitazone (10 μM), or control (0.5% dimethyl sulfoxide) were treated for 1 h before being treated with TNFα at a concentration of 10 ng/mL for 15 h. Data are expressed as means ± standard error of the mean (n = 8). Values without a common letter are significantly different at the $P < 0.05$ level.

hexane as an eluent to provide amide **8** (94.5 mg, 42%): ^{1}H NMR δ 0.035 (s, 3H), 0.047 (s, 3H), 0.80 (s, 9H), 0.88 (t, 3H, J = 6.9 Hz), 1.3−1.5 (8H), 2.31 (dd, 1H, J = 14.7 Hz, J = 5.1 Hz), 2.47 (dd, 1H, J = 14.7 Hz, J = 4.2 Hz), 3.87 (s, 3H), 4.01 (m, 1H), 4.23 (dd, 1H, J = 14.3 Hz, J = 5.1 Hz), 4.50 (dd, 1H, J = 14.3 Hz, J = 6.0 Hz), 6.77 (dd, 1H, J = 8.06 Hz, J = 1.83 Hz), 6.80 (d, 1H, J = 1.83 Hz), 6.85 (d, 1H, J = 8.06 Hz); ^{13}C NMR δ −4.90, −4.76, 13.9, 17.7, 22.5, 25.1, 25.6, 31.7, 36.6, 43.4, 55.8, 69.7, 110.9, 114.5, 120.9, 130.0, 145.1, 146.7, 174.0; IR (neat) 3306.7 (br), 2955.6 (m), 2930.0 (s), 2857.4 (m), 1651.7 (s), 1516.7 (s), 1463.5 (m), 1432.9 (w), 1378.3 (w), 1255.9 (m), 836.5 (w), 776.5 (w) cm^{-1}; HRMS (ESI) m/z calcd for $C_{22}H_{39}NO_4SiNa$ $(M + Na)^+$ 432.2546, found 432.2564.

3-Hydroxy-*N*-(4-hydroxy-3-methoxybenzyl)octanamide (2). To a solution of **7** (92.1 mg, 0.22 mmol) in CH_2Cl_2 (2.2 mL) was added *p*-toluenesulfonic acid (0.129 g, 0.68 mmol), and the mixture was stirred for 2 h. A saturated aqueous $NaHCO_3$ solution was added to the mixture, and the mixture was extracted with dichloromethane. The extract was dried over anhydrous magnesium sulfate, filtered, and condensed in vacuo. The residue was chromatographed on silica gel with a 2:1 ethyl acetate/hexane solution as an eluent to provide **2** (47.0 mg, 72%): ^{1}H NMR δ 0.88 (t, 3H, J = 6.6 Hz), 1.3−1.5 (8H), 2.27 (dd, 1H, J = 15.2 Hz, J = 8.8 Hz), 2.38 (dd, 1H, J = 15.2 Hz, J = 2.9 Hz), 4.00 (m, 1H), 4.36 (d, 1H, J = 5.5 Hz), 6.77 (dd, 1H, J = 7.7 Hz, J = 1.7 Hz), 6.80 (d, 1H, J = 1.7 Hz), 6.87 (d, 1H, J = 7.7 Hz); ^{13}C NMR δ 23.7, 32.2, 34.8, 41.4, 46.6, 52.2, 53.1, 65.6, 78.5, 120.4, 124.2, 130.4, 139.5, 154.8, 156.5, 182.0; IR (neat) 3318.7 (br), 2930.7 (m), 2857.6 (s), 1638.2 (s), 1550.3 (w), 1517.1 (s), 1464.3 (m), 1431.8 (w), 1238.6 (w), 1277.0 (m), 1034.8 (m), 835.2 (w), 798.5 (w) cm^{-1}; MS (FAB) M = 295.2, 296.2 (M + 1); HRMS (ESI) m/z calcd for $C_{16}H_{25}NO_4Na$ $(M + Na)^+$ 318.1681, found 318.1692.

Animals. Male Jcl:MCH (ICR) mice [n = 21, body weight of 27−30 g, 6 weeks of age (CLEA Japan, Tokyo, Japan)] were used in this study. The animal room had a controlled temperature of 22 ± 2 °C, a humidity of 60 ± 5%, and a 12 h−12 h light−dark cycle (i.e., lights on from 8:00 a.m. to 8:00 p.m.); the animals were given food and water *ad libitum*, or as otherwise noted. The light intensity at the surface of the cages was approximately 100 lx. Mice were fed either a control regular rodent chow, i.e., 63% carbohydrate, 5% fat, and 32% protein (CE-2, CLEA Japan), or a high-fat diet, i.e., 25% beef tallow (w/w) added to the regular rodent chow (Oriental Yeast Co., Ltd.), or a high-fat diet supplemented with 0.06% 6G or A6G for 86 days. The animal experiments were conducted under the permission of the Animal Welfare Committee of Waseda University (Permission 10A35).

Experimental Protocol. The mice were randomly divided into groups of 6 each on day 0. The fasting blood glucose level was measured after animals had fasted for 12 h (starting from 8:00 p.m.) on day 0 (before treatment), 9, 16, 23, 30, 44, 48, 57, 68, and 86. On day 90, MRI was performed. On days 92−94, an oral glucose tolerance test (OGTT) was performed after overnight fasting. Blood was sampled from the tail vein of mice at 0 min (baseline) and 30, 60, 120, and 240 min after an oral glucose load of 3.0 g/kg of body weight. Food, but not water, was withheld from the cages during the OGTT test. Blood glucose levels were measured by Glucose Pilot (Aventir Biotech, LLC) as per the manufacturer's instructions. On day 100, after having fasted for 12 h, the mice from the four groups (HFD, RC, HFD with A6G, and HFD with 6G) were sacrificed; the visceral and subcutaneous fat and liver were dissected, and blood samples were collected. Plasma samples were stored at −20 °C for the determination of insulin and leptin levels using the mouse insulin ELISA kit (Shibayagi Co., Ltd., Gunma, Japan) and the mouse leptin ELISA kit (R&D, Minneapolis, MN), respectively, according to the manufacturers' instructions. The visceral fat obtained from each mouse was dissected and weighed. A small portion of the liver and the visceral fat from each mouse was dissolved in phenol (Omega Biotek, Inc.).

RNA Isolation and Real-Time RT-PCR. Total RNA was extracted using the phenol-dissolved samples. Here, 50 ng of total RNA was reverse transcribed and amplified using the One-Step SYBR RT-PCR Kit (TaKaRa, Otsu, Japan) in the Step One Plus Real-Time PCR System (Applied Biosystems, Foster City, CA). Specific primer pairs were designed using Primer3 Input (version 0.4.0). The following primers were used: β-actin-F, 5′-TGACAGGATGCAGAAGGAGA-3′;

β-actin-R, 5′-GCTGGAAGGTGGACAGTGAG-3′; Gapdh-F, 5′-TGGTGAAGGTCGGTGTGAAC-3′; Gapdh-R, 5′-AATGAAGGGGTCGTTGATGG-3′; TNFα-F, 5′-ATCCGCGACGTGGAACTG-3′; TNFα-R, 5′-ACCGCCTGGAGTTCTGGAA-3′; leptin-F, 5′-TCACACACGCAGTCGGTATC-3′; leptin-R, 5′-GCTGGTGAGGACCTGTTGATAG-3′; SREBP-1c-F, 5′-CGCTACCGGTCTTCTATCAATG-3′; SREBP-1c-R, 5′-CAAGAAGCGGATGTAGTCGATG-3′; ACCα-F, 5′-CATGAACACCCAGAGCATTG-3′; ACCα-R, 5′-ATTTGTCGTAGTGGCCGTTC-3′; FAS-F, 5′-GGCAGAGAAGAAAGCTGTGG-3′; and FAS-R, 5′-TCGGATGCCTAGGATGTGTG-3′ [with forward (F), reverse (R), glyceraldehyde-3-phosphate dehydrogenase (GAPDH), tumor necrosis factor (TNF), acetyl-CoA (ACC), and fatty acid synthase (FAS)]. RT-PCR was performed under the following conditions: cDNA synthesis at 42 °C for 15 min followed by 95 °C for 2 min, PCR amplification for 40 cycles with denaturation at 95 °C for 5 s, and annealing and extension at 60 °C for 20 s. The relative light unit of the target gene PCR products was normalized to that of β-actin for liver samples or Gapdh for adipose tissue samples. Melting curve analysis was then performed. The specificity of gene amplification was confirmed by measuring the size and purity of the PCR product by gel electrophoresis.

3T3-L1 Cell Culture and Treatment. Mouse 3T3-L1 cells were purchased from DS Pharma Biomedical Co., Ltd. (Osaka, Japan). These cells were cultured in preadipocyte maintenance medium (DS Pharma Biomedical) at 37 °C in 5% CO_2. Confluent cells were placed in a differentiation medium (DS Pharma Biomedical) for 3 days. The medium was then changed to adipocyte maintenance medium (DS Phama Biomedical). Seven days after the differentiation of preadipocytes into adipocytes, these adipocytes were pretreated with 6G, A6G, rosiglitazone (rosiglitazone is a thiazolidinedione that has been shown to be highly effective in reducing insulin resistance and improving type 2 diabetes) (Wako Pure Chemical Industries, Ltd., Osaka, Japan) or vehicles (0.5% dimethyl sulfoxide) for 1 h. Then the cells were treated with TNFα [10 ng/mL (Sigma-Aldrich, St. Louis, MO)] for 15 h. After treatment, the total RNA from the adipocytes was isolated using the QIAzol TM reagent (QIAGEN, Tokyo, Japan) according to the manufacturer's directions. cDNA was prepared from 1 μg of total RNA using reverse transcriptase [Superscript III (Invitrogen)]. The quantification of gene expression in the adipocytes was measured using TaqMan Gene Expression Assays (mouse adiponectin, Mm00456425_m1; mouse β-actin, 4352933E), the TaqMan fast advanced master mix core reagent kit, and ABI Prism 7900 (Applied Biosystems). The gene expression level was evaluated by the $2(-\Delta\Delta C(T))$ method.[37] The gene expression level was expressed relative to the control (1.0) after normalization using the β-actin gene expression level.

Magnetic Resonance Imaging. An exact quantification of fat distribution was performed by MRI as previously described by Machann et al.[38,39] MRI-derived visceral (VS) fat, subcutaneous (SC) fat, and total body fat masses are represented in milligrams. The mice were imaged on a 0.4 T open MRI system (Hitachi Medico Ltd., Tokyo, Japan) using a custom-designed send−receive coil assembled to take high-resolution images. This is a solenoid-type system, and its resonance frequency is tuned to fit that of the MRI system using a network analyzer. Using this coil, a clearer image can be obtained compared to that obtained using conventional MRI receiver coils. The experimental animal was administered an anesthetic before being placed into the MRI and then into the coil. Axial spin-echo T1-weighted sequences were obtained for the entire mouse (head to anus). The distribution of the fat was visualized with Osirix version 3.9. Volumes of the VS and SC fats and the whole body of the animal were measured using three-dimensional (3D) volume-rendering software (Mimics 13.0, Materialize). The procedure can be described in the following three steps: (1) areas of fat and the whole body extracted and binarized using the binarizing function provided by the software with a threshold for fat, (2) volumes of the fats and the whole body calculated using the 3D volume rendering function provided by the software, and (3) percent body fat calculated.

Statistical Analyses. The data were expressed as means ± standard error of the mean. The differences among the means were analyzed by a Tukey-Kramer test following one-way ANOVA. Differences in P values of <0.05 were considered statistically significant. All the statistical analyses were performed using StatView version 5.0 (SAS Institute Inc., Cary, NC).

AUTHOR INFORMATION

Corresponding Author

*Phone: +81-3-5286-3205. Fax: +81-3-3232-5270. E-mail: okamoto@aoni.waseda.jp.

ACKNOWLEDGMENT

The MRI receiving coil was developed with the support by Prof. Iseki and Dr. Suzuki (Tokyo Women's Medical University, Tokyo, Japan). This research was supported by the Supporting Project to Form the Strategic Research Platforms for Private University and a Matching Fund Subsidy from the Ministry of Education, Culture, Sports, Science and Technology (MEXT), Japan.

ABBREVIATIONS USED

HFD, high-fat diet; RC, regular chow; SREBP, sterol regulatory element-binding protein; HDL, high-density lipoprotein; LDL, low-density lipoprotein; ACC, acetyl-CoA carboxylase; FAS, fatty acid synthase; STZ, streptozotocin; TRPV1, transient receptor potential vanilloid-1; MRI, magnetic resonance imaging; CT, computed tomography; OGTT, oral glucose tolerance test; VS, visceral; SC, subcutaneous; TNFα, tumor necrosis factor-α; PPAR-γ, peroxisome proliferator-activated receptor-γ; JNK, Jun-N-terminal kinase

REFERENCES

(1) Harwood, H. J., Jr. Treating the metabolic syndrome: Acetyl-CoA carboxylase inhibition. *Expert Opin. Ther. Targets* **2005**, *9*, 267–281.

(2) Kusunoki, J.; Kanatani, A.; Moller, D. E. Modulation of fatty acid metabolism as a potential approach to the treatment of obesity and the metabolic syndrome. *Endocrine* **2006**, *29*, 91–100.

(3) Abu-Elheiga, L.; Oh, W.; Kordari, P.; Wakil, S. J. Acetyl-CoA carboxylase 2 mutant mice are protected against obesity and diabetes induced by high-fat/high-carbohydrate diets. *Proc. Natl. Acad. Sci. U.S.A.* **2003**, *100*, 10207–10212.

(4) Choi, C. S.; Savage, D. B.; Abu-Elheiga, L.; Liu, Z. X.; Kim, S.; Kulkarni, A.; Distefano, A.; Hwang, Y. J.; Reznick, R. M.; Codella, R.; Zhang, D.; Cline, G. W.; Wakil, S. J.; Shulman, G. I. Continuous fat oxidation in acetyl-CoA carboxylase 2 knockout mice increases total energy expenditure, reduces fat mass, and improves insulin sensitivity. *Proc. Natl. Acad. Sci. U.S.A.* **2007**, *104*, 16480–16485.

(5) Cool, B.; Zinker, B.; Chiou, W.; Kifle, L.; Cao, N.; Perham, M.; Dickinson, R.; Adler, A.; Gagne, G.; Iyengar, R.; Zhao, G.; Marsh, K.; Kym, P.; Jung, P.; Camp, H. S.; Frevert, E. Identification and characterization of a small molecule AMPK activator that treats key components of type 2 diabetes and the metabolic syndrome. *Cell Metab.* **2006**, *3*, 403–416.

(6) Kim, M. S.; Park, J. Y.; Namkoong, C.; Jang, P. G.; Ryu, J. W.; Song, H. S.; Yun, J. Y.; Namgoong, I. S.; Ha, J.; Park, I. S.; Lee, I. K.; Viollet, B.; Youn, J. H.; Lee, H. K.; Lee, K. U. Anti-obesity effects of α-lipoic acid mediated by suppression of hypothalamic AMP-activated protein kinase. *Nat. Med.* **2004**, *10*, 727–733.

(7) Awang, D. Ginger. *Can. Pharm. J.* **1992**, *125*, 309–311.

(8) Tapsell, L. C.; Hemphill, I.; Cobiac, L.; Patch, C. S.; Sullivan, D. R.; Fenech, M.; Roodenrys, S.; Keogh, J. B.; Clifton, P. M.; Williams, P. G.; Fazio, V. A.; Inge, K. E. Health benefits of herbs and spices: The past, the present, the future. *Med. J. Aust.* **2006**, *185*, S4–S24.

(9) Wang, W. H.; Wang, Z. M. [Studies of commonly used traditional medicine-ginger]. *Zhongguo Zhong Yao Za Zhi* **2005**, *30*, 1569–1573.

(10) Govindarajan, V. Ginger-chemistry technology and quality evaluation: Part 2. *Crit. Rev. Food Sci. Nutr.* **1982**, *17*, 189–258.

(11) Govindarajan, V. Ginger-chemistry technology and quality evaluation: Part 1. *Crit. Rev. Food Sci. Nutr.* **1982**, *17*, 1–96.

(12) Connell, D. W.; Sutherland, M. D. A Re-examination of gingerol shogaol and zingerone pungent principles of ginger (*Zingiber officinale* Roscoe). *Aust. J. Chem.* **1969**, *22*, 1033–1043.

(13) Isa, Y.; Miyakawa, Y.; Yanagisawa, M.; Goto, T.; Kang, M. S.; Kawada, T.; Morimitsu, Y.; Kubota, K.; Tsuda, T. 6-Shogaol and 6-gingerol, the pungent of ginger, inhibit TNF-α mediated downregulation of adiponectin expression via different mechanisms in 3T3-L1 adipocytes. *Biochem. Biophys. Res. Commun.* **2008**, *373*, 429–434.

(14) Ali, B. H.; Blunden, G.; Tanira, M. O.; Nemmar, A. Some phytochemical, pharmacological and toxicological properties of ginger (*Zingiber officinale* Roscoe): A review of recent research. *Food Chem. Toxicol.* **2008**, *46*, 409–420.

(15) Al-Amin, Z. M.; Thomson, M.; Al-Qattan, K. K.; Peltonen-Shalaby, R.; Ali, M. Anti-diabetic and hypolipidaemic properties of ginger (*Zingiber officinale*) in streptozotocin-induced diabetic rats. *Br. J. Nutr.* **2006**, *96*, 660–666.

(16) Iwasaki, Y.; Morita, A.; Iwasawa, T.; Kobata, K.; Sekiwa, Y.; Morimitsu, Y.; Kubota, K.; Watanabe, T. A nonpungent component of steamed ginger-[10]-shogaol increases adrenaline secretion via the activation of TRPV1. *Nutr. Neurosci.* **2006**, *9*, 169–178.

(17) Luo, X. J.; Peng, J.; Li, Y. J. Recent advances in the study on capsaicinoids and capsinoids. *Eur. J. Pharmacol.* **2011**, *650*, 1–7.

(18) Calderan, L.; Marzola, P.; Nicolato, E.; Fabene, P. F.; Milanese, C.; Bernardi, P.; Giordano, A.; Cinti, S.; Sbarbati, A. In vivo phenotyping of the ob/ob mouse by magnetic resonance imaging and ^{1}H-magnetic resonance spectroscopy. *Obesity* **2006**, *14*, 405–414.

(19) Gronemeyer, S. A.; Steen, R. G.; Kauffman, W. M.; Reddick, W. E.; Glass, J. O. Fast adipose tissue (FAT) assessment by MRI. *Magn. Reson. Imaging* **2000**, *18*, 815–818.

(20) Iacobellis, G. Imaging of visceral adipose tissue: An emerging diagnostic tool and therapeutic target. *Curr. Drug Targets: Cardiovasc. Haematol. Disord.* **2005**, *5*, 345–353.

(21) Ross, R.; Leger, L.; Guardo, R.; Deguise, J.; Pike, B. G. Adipose-tissue volume measured by magnetic-resonance-imaging and computerized-tomography in rats. *J. Appl. Physiol.* **1991**, *70*, 2164–2172.

(22) Walling, B. E.; Munasinghe, J.; Berrigan, D.; Bailey, M. Q.; Simpson, R. M. Intra-abdominal fat burden discriminated in vivo using proton magnetic resonance spectroscopy. *Obesity* **2007**, *15*, 69–77.

(23) Ferre, P.; Foufelle, F. SREBP-1c transcription factor and lipid homeostasis: Clinical perspective. *Horm. Res.* **2007**, *68*, 72–82.

(24) Shimano, H. SREBPs: Physiology and pathophysiology of the SREBP family. *FEBS J.* **2009**, *276*, 616–621.

(25) Riccardi, G.; Giacco, R.; Rivellese, A. A. Dietary fat, insulin sensitivity and the metabolic syndrome. *Clin. Nutr.* **2004**, *23*, 447–456.

(26) Fujimoto, W. Y. The importance of insulin resistance in the pathogenesis of type 2 diabetes mellitus. *Am. J. Med.* **2000**, *108* (Suppl. 6a), 9S–14S.

(27) Edelman, S. V. Type II diabetes mellitus. *Adv. Intern. Med.* **1998**, *43*, 449–500.

(28) Fernandez, M. L. The metabolic syndrome. *Nutr. Rev.* **2007**, *65*, S30–S34.

(29) Buettner, R.; Parhofer, K. G.; Woenckhaus, M.; Wrede, C. E.; Kunz-Schughart, L. A.; Scholmerich, J.; Bollheimer, L. C. Defining high-fat-diet rat models: Metabolic and molecular effects of different fat types. *J. Mol. Endocrinol.* **2006**, *36*, 485–501.

(30) Buettner, R.; Scholmerich, J.; Bollheimer, L. C. High-fat diets: Modeling the metabolic disorders of human obesity in rodents. *Obesity* **2007**, *15*, 798–808.

(31) Singh, A. B.; Akanksha; Singh, N.; Maurya, R.; Kumar, A.; Srivastava Anti-hyperglycaemic, lipid lowering and anti-oxidant properties of [6]-gingerol in db/db mice. *Int. J. Med. Med. Sci.* **2009**, *1*, 546–544.

(32) Nammi, S.; Sreemantula, S.; Roufogalis, B. D. Protective effects of ethanolic extract of *Zingiber officinale* rhizome on the development of metabolic syndrome in high-fat diet-fed rats. *Basic Clin. Pharmacol. Toxicol.* **2009**, *104*, 366–373.

(33) Mustafa, T.; Srivastava, K. C.; Jensen, K. B. Drug development report: 9. Pharmacology of ginger, *Zingiber officinale*. *J. Drug Dev.* **1993**, *6*, 25–39.

(34) Bhattarai, S.; Tran, V. H.; Duke, C. C. Stability of [6]-gingerol and [6]-shogaol in simulated gastric and intestinal fluids. *J. Pharm. Biomed. Anal.* **2007**, *45*, 648–653.

(35) Kuwajima, I.; Minami, N.; Sato, T. Convenient method for preparation of β-hydroxy esters. *Tetrahedron Lett.* **1976**, 2253–2256.

(36) Kiyooka, S.; Hena, M. A. A study directed to the asymmetric synthesis of the antineoplastic macrolide acutiphycin under enantioselective acyclic stereoselection based on chiral oxazaborolidinone-promoted asymmetic aldol reactions. *J. Org. Chem.* **1999**, *64*, 5511–5523.

(37) Livak, K. J.; Schmittgen, T. D. Analysis of relative gene expression data using real-time quantitative PCR and the 2(T)($-\Delta\Delta$C) method. *Methods* **2001**, *25*, 402–408.

(38) Machann, J.; Thamer, C.; Schnoedt, B.; Haap, M.; Haring, H. U.; Claussen, C. D.; Stumvoll, M.; Fritsche, A.; Schick, F. Standardized assessment of whole body adipose tissue topography by MRI. *J. Magn. Reson. Imaging* **2005**, *21*, 455–462.

(39) Machann, J.; Thamer, C.; Schnoedt, B.; Stefan, N.; Stumvoll, M.; Haring, H. U.; Claussen, C. D.; Fritsche, A.; Schick, F. Age and gender related effects on adipose tissue compartments of subjects with increased risk for type 2 diabetes: A whole body MRI/MRS study. *Magn. Reson. Mater. Phys., Biol. Med.* **2005**, *18*, 128–137.